Journal of Sound and Vibration (1997) **203**(2), 237–249

THE DYNAMIC ANALYSIS OF A THIN BEAM IMPACTING AGAINST A STOP OF GENERAL THREE-DIMENSIONAL GEOMETRY

C. WANG† AND J. KIM

Structural Dynamics Research Laboratory, Mechanical Engineering Department, University of Cincinnati, Cincinnati, OH 45221-0072, *U.S.A.*

(*Received* 26 *June* 1996, *and in final form* 18 *November* 1996)

The dynamic response of a thin cantilever beam impacting against an elastic stop of general three-dimensional geometry is studied by extending the analysis procedure developed in the authors' previous work [1]. For the impulse response functions of the beam and stop required by the analysis procedure, an analytic solution is used for the beam and a finite element method solution is used for the stop. The contact area between the beam and the stop is the only parameter that has to be assumed in the procedure. While changes to this parameter result in significant changes to the estimate of the contact force, it is shown that at a point relatively far from the contact center the dynamic response is influenced only slightly by the assumed area. This may be interpreted as a dynamic version of the Saint-Venant's principle. It should be noted that fatigue failures of thin beams usually occur near the free edge, relatively far from the contact point, where the stress wave is reflected. Therefore, impact analysis of a thin beam against a three-dimensional object can be performed in a self contained manner for most practical purposes. Characteristics of the dynamic response of systems with a stop of various geometry are discussed based on numerical results.

1. INTRODUCTION

Automatic valve systems found in many practical applications such as refrigeration compressors or small engines are composed of a thin plate which resembles a cantilever beam and a stop of an arbitrary three-dimensional geometry. When elastic impact problems between a thin beam and a stop were solved in the past [2–4], an equivalent linear spring had been used to model the latter. In the authors' previous work [1], it was shown that such an approach is valid only when all key dimensions of the stop are significantly smaller when compared to the width or length of the beam. Thus, the existing approach leads to an erroneous result as the size of the stop becomes large, as occurs in most practical cases, because the dynamics of the stop are as important as that of the beam for these cases. In the new solution procedure proposed by the authors, the impulse response functions of the beam and the stop are utilized to include fully the dynamics of both the beam and the stop in the analysis. Applicaton of the procedure was demonstrated for systems with a stop of one-dimensional geometry in reference [1].

However, virtually all valve stops in practical applications have a geometry that should be modelled as a three-dimensional object. Our literature survey did not find any reported work on the analysis of the impact between a thin beam and a three-dimensional elastic

† Currently with Center for Industrial Safety and Health Technology, Industrial Technology Research Institute (ITRI), Chutung, Hsinchu, Taiwan, Republic of China.

0022–460X/97/220237 + 13 $25.00/0/sv960875

object. With a similar motivation as this work, namely design analysis of valve failures, some authors solved for the stress wave propagation in the elastic medium. Blinka solved stress wave propagation problems in the two-dimensional half space [5]. Kim and Soedel solved for the elastic wave propagation in a three-dimensional half space [6] and in a finite thickness plate [7] by the method of superposition of the dynamic Green's function. However, the dynamics of the beam were not considered in their works, where the impact load acting on the stop was assumed to be known.

Since no analytic solutions are available for the impulse response functions of general three-dimensional objects, the finite element method (FEM) is used to obtain the impulse response function of the stop. It is realized that the contact area between the beam and the stop has to be assumed in the procedure developed in reference [1] when it is applied to the problems with a stop of three-dimensional geometry. For the system with a one-dimensional stop studied in reference [1], the contact area was simply given as the cross-sectional area of the rod, therefore no assumed parameter had to be used. Analytical results of the beam impacting against a three-dimensional half space show that the contact pressure time history calculated from the procedure strongly depends on the size of this contact area, an arbitrarily assumed parameter. This may raise a doubt about the value of using the analytical procedure proposed in reference [1] for three-dimensional problems. However, further study reveals that the dynamic response at a point relatively far from the contact center is influenced only slightly by the assumed contact area value, therefore analysis of the impact between a thin beam and a three-dimensional object can be conducted in a consistent manner if the main concern is not the close vicinity of the contact center.

2. SOLUTION PROCEDURE

Figure 1 is an illustration of the problem considered in this work. A thin cantilever beam with an initial tip deflection δ_0 is released from rest to hit a stop of general three-dimensional geometry. In the authors' previous work [1], a solution procedure was proposed to solve such an impact problem fully considering the dynamics of both the beam and the stop. The procedure is briefly summarized here.

The motion of the beam after the release can be described as

$$y(x, t) = y_h(x, t) + \int_0^t g_b(x, t - \tau)F(\tau)\,\mathrm{d}\tau, \tag{1}$$

where x is the co-ordinate attached to the beam, $y_h(x, t)$ is the homogeneous solution representing the initial transient motion, and the convolution integral part is the forced response to the contact force. Also, $g_b(x, t)$ is the impulse response function of the beam which is defined as the beam displacement in response to a unit impulse load applied at

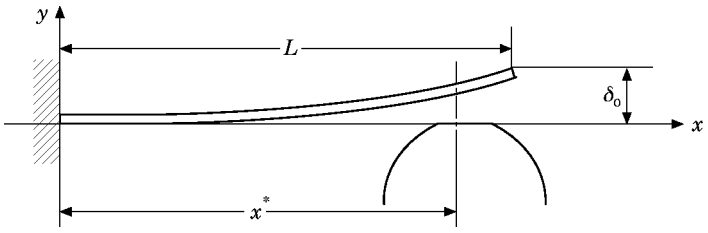

Figure 1. Illustration of the problems to be discussed.

the contact point x^*, $F(t)$ is the contact force resulting from the impact. The initial time $t = 0$ is taken as the instant when the initial contact starts.

The motion of the stop can also be described in a similar way as follows:

$$u(\tilde{\mathrm{r}}, t) = -\int_0^t g_s(\tilde{\mathrm{r}}, t-\tau)F(\tau)\,\mathrm{d}\tau, \tag{2}$$

where $\tilde{\mathrm{r}}$ is the position vector according to the co-ordinate system that describes the geometry of the stop, and $g_s(\tilde{\mathrm{r}}, t)$ is the impulse response of the stop which is defined as the displacement of the stop induced by a unit impulse load input at the contact point $\tilde{\mathrm{r}}^*$. The free vibration term is not included in equation (2) since the stop is assumed to be at rest before the contact occurs.

The impulse responses of the beam and the stop are defined as their displacement responses to a unit impulse force input at the contact point. If both impulse response functions are known, equations (1) and (2) can be integrated simultaneously to obtain the contact force by applying the following conditions.

if $y(x^*, t) > u(\tilde{\mathrm{r}}^*, t)$, set $F(t) = 0$ (no contact). $y(x^*, t)$ and $u(\tilde{\mathrm{r}}^*, t)$ at the next time step are calculated separately by the numerical integrations described by equations (1) and (2).

if $y(x^*, t) \leqslant u(\tilde{\mathrm{r}}^*, t)$, set $y(x^*, t) \equiv u(\tilde{\mathrm{r}}^*, t)$ (contact in progress). The contact force is calculated as follows [1]:

$$F(t) = -\frac{y_b(x^*, t) + \int_0^{t-\Delta t} F(\tau)g_b(x^*, t-\tau)\,\mathrm{d}\tau + \int_0^{t-\Delta t} F(\tau)g_s(\tilde{\mathrm{r}}^*, t-\tau)\,\mathrm{d}\tau}{[g_b(x^*, \Delta t) + g_s(\tilde{\mathrm{r}}^*, \Delta t)]\Delta t}, \tag{3}$$

where Δt is the time step used in the integration.

Integrations in equations (1) and (2) are continued using the contact force calculated from equation (3) to find the displacements of the beam and the stop at the next time step.

The procedure goes back to the first step and continues.

As the result of the above procedure, the time histories of the contact force and displacements of the stop and the beam at the contact point are calculated. Utilizing the contact force time history found, dynamic responses of the beam and the stop at any points can be obtained from equations (1) and (2), respectively. Detailed discussions on the actual numerical implementation of the procedure can be found in reference [1].

3. IMPULSE RESPONSE FUNCTIONS

If the impulse response functions of the beam and the stop are known, the impact analysis procedure explained above becomes a fairly straightforward numerical task. An analytic solution is used as the response function of the beam and a FEM solution is used as the response function of the stop.

3.1. IMPULSE RESPONSE FUNCTION OF THE BEAM

The impulse response function of the beam $g_b(x, t)$ can be obtained by solving the following equation.

$$EI(\partial^4 y/\partial x^4) - \rho A\,\partial^2 y/\partial t^2 = 1 \cdot \delta(t)\delta(x - x^*) \tag{4}$$

where y is the beam deflection, E is the Young's modulus of the beam material, I is the mass moment of inertia of the beam section, ρ is the mass density, A is the cross-sectional area of the beam, $\delta(x)$ and $\delta(t)$ are Dirac delta functions in spatial and temporal domains, respectively. The impulse response function of the beam can be obtained by the modal expansion method as it was done in reference [1]. The function is obtained as

$$g_b(x, t) = \sum_{n=1}^{n_b} \frac{\phi_n(x)}{m\omega_n} \phi_n(x^*) \sin \omega_n t, \tag{5}$$

where m is the total mass of the beam, n_b is the number of beam modes used in the expansion, ϕ_n and ω_n are the nth natural mode and natural frequency of the clamped-free beam, respectively.

3.2. IMPULSE RESPONSE FUNCTION OF THE STOP

The impulse response function of the stop $g_s(\check{\mathrm{r}}, t)$ is the displacement response of the stop to the unit impulse force input that can be described by two Dirac delta functions as follows:

$$F(\check{\mathrm{r}}, t) = 1 \cdot \delta(t)\delta(\check{\mathrm{r}} - \check{\mathrm{r}}^*), \tag{6}$$

where $\check{\mathrm{r}}^*$ is the position vector of the contact point. The finite element method is utilized in this work according to the procedure to be described in the following.

For the numerical implementation, the time domain Dirac delta function $\delta(t)$ is approximated as a very narrow gate function. That is,

$$\delta(t - t^*) = 0, \quad \text{for} \quad t < t^*, = 1/\Delta t, \quad \text{for} \quad t^* < t < t^* + \Delta t, = 0, \quad \text{for} \quad t > t^* + \Delta t. \tag{7}$$

Further, the gate function in equation (7) is obtained as a superposition of two unit step functions:

$$\delta(t - t^*) = (1/\Delta t)(\hat{U}(t - t^*) - \hat{U}(t - (t^* + \Delta t))). \tag{8}$$

This method, superposing two step functions, allows the width of the gate function which approximates the Dirac delta functions to be made as small as one integration time step.

In the spatial domain, the Dirac delta function $\delta(\check{\mathrm{r}} - \check{\mathrm{r}}^*)$ is approximated as a uniformly distributed pressure load over a small circle centered at the contact point, whose total magnitude is 1 N. Again, this can be represented as a superposition of two unit step functions in the spatial domain as

$$\delta(r - r^*) = (1/\pi\varepsilon^2)(\hat{U}(r) - \hat{U}(r - \varepsilon)), \tag{9}$$

where, ε is the radius of the circle representing the contact area.

Utilizing the linearity of the problem being discussed in conjunction with the above expressions, the impulse response function of a three-dimensional object can be obtained as follows. (1) Calculate the response of the stop using its FEM model when it is subjected to a pressure load defined by equation (9) in the spatial domain, applied as a unit step function in the time domain. The calculated response is stored as a form of discrete numerical series. (2) Shift the numerical series representing the displacement solution by one time step. (3) Subtract two series and divide the result by the time step size.

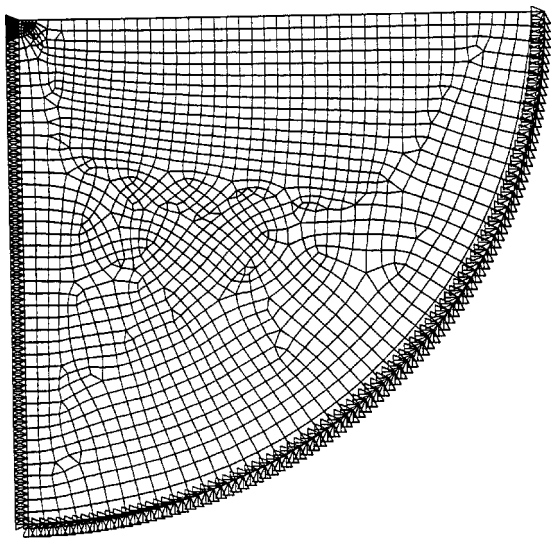

Figure 2. FEM model of the half space.

4. IMPACT OF THE BEAM AGAINST A HALF SPACE

At first, the analysis procedure is applied to analyze when a thin beam impacts against a half space. It is assumed that the location of the contact point remains the same during the progress of the contact process. The material properties of the beam, the Young's modulus, Poisson's ratio and mass density are taken as 70×10^9 N/m^2, 0·3 and 2780 kg/m^3, respectively, which corresponds to the properties of aluminum. The length, the width and the thickness of the beam used in the calculation are 10 mm, 60 mm and 1 mm, respectively. The contact point is assumed to be at the free end of the beam and the initial deflection of the beam δ_0 is taken as 10 mm.

4.1. IMPULSE RESPONSE OF THE HALF SPACE

Figure 2 shows the FEM model used to obtain the impulse response function of the half space. The radius of the contact circle ε is taken as 1 mm and the radius of the circle representing the half space R is taken as 60 mm. The latter is taken large enough compared to the former to make the effect of the wave reflection from the boundary negligible during the progress of the impact so that the half space condition can be approximated. The material properties of the half space are taken to be the same as the beam.

The displacement time histories of the half space on the free surface in response to a unit step input force from the FEM analysis is shown in Figure 3. Figure 4 shows the surface deflection of the half space at 7·5 μs after the unit step force was applied compared with the static deflection obtained from the exact solution in reference [8]. The wave front is observed approximately at $r = 9$ mm in the figure. The two solutions are almost identical in the region which the wave front passed which shows that the FEM mesh used to obtain the step response is detailed enough to provide an accurate result.

The impulse response function obtained by superposing two step responses as explained in section 3.2. is shown in Figure 5. The two unit step responses are shifted by a single time step of the numerical integration, the displacement response rises to approximately the maximum value immediately at the first integration time step. The analytic impulse response at the contact point, if it were available, would have shown an instantaneous response judging from the exact solution for a one-dimensional rod case discussed in

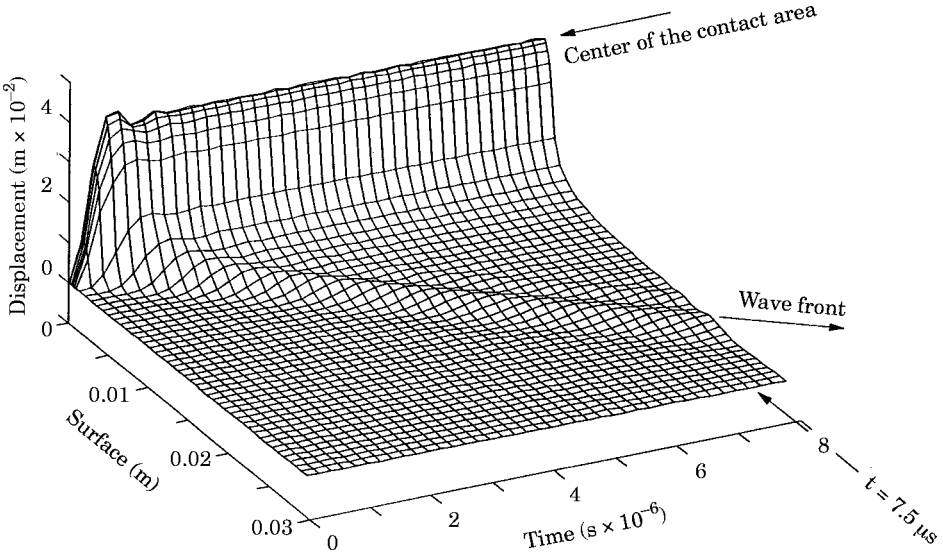

Figure 3. Half space response to a unit step input force.

reference [1]. It is necessary to ensure that this rise time is equal to the integration time step to have a correct converged impact force time history, as also discussed in reference [1].

4.2. IMPACT FORCE TIME HISTORY AND THE EFFECT OF THE ASSUMED CONTACT AREA

Figure 6 shows the time history of the contact force between the beam and the half space calculated according to the procedure explained previously.

As was mentioned, the radius of the contact circle ϵ has to be assumed as an arbitrary small value in the analysis procedure. In Figure 7, the time histories of the calculated contact pressure are compared for the same system that was used to obtain Figure 6 when two different radii of the contact circle, 1 mm and 2 mm, are used. The large discrepancy between these two estimations may raise a doubt about the value of the proposed procedure since a different assumed area results in a significantly different estimated impact force. This problem was not encountered when the system has a one-dimensional

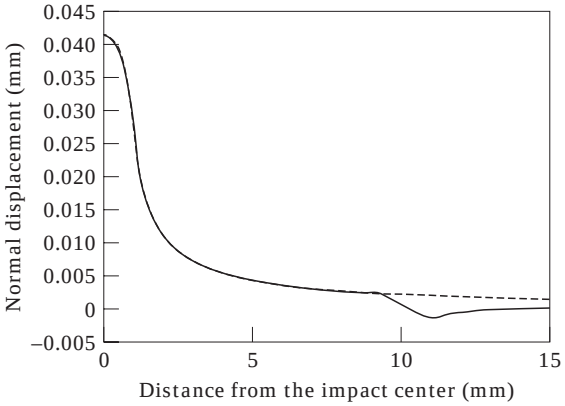

Figure 4. Surface deflection of the half space: (——), dynamic response at $t = 7.5\ \mu$s; - - - - -, static response.

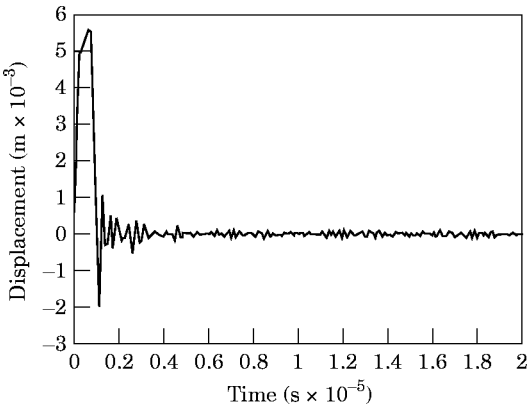

Figure 5. Impulse response function of the half space.

stop geometry as demonstrated in the authors' previous work [1] because the contact area was simply given as the cross-sectional area of the rod in such cases.

In the following section, it is shown that this is not a severe limitation in practical applications because the response at a point very close to the contact center is usually not of main concern. For example, most figure failures observed in a thin cantilever beam used as an automatic reed valve in compressors or small engines occur near the free edge, relatively far from the contact point. This is caused by the instantaneous change of the state of the stress wave, from compression to tension, when it is reflected at the free edge.

4.3. DYNAMIC VERSION OF THE SAINT-VENANT'S PRINCIPLE

The dynamic responses at the points relatively far from the contact center, when different contact areas are assumed, allows one to see the effect of this parameter. The displacement time histories are compared in Figure 8 for the same two contact radii as those used to make Figure 7, $\varepsilon = 1$ mm and $\varepsilon = 2$ mm, at the points 2·5 mm, 5 mm, 10 mm and 15 mm from the center of the contact. These points lie on the free surface of the half space. As the figure indicates, the responses of the two cases become closer to each other as the point of comparison moves to a point farther away from the contact center. The two simulated response signals become fairly close to each other at the points away from the contact center by 10 mm or more. Figure 9 shows the same phenomenon presented in terms of the stress intensities. This suggests that, at the points relatively far from the

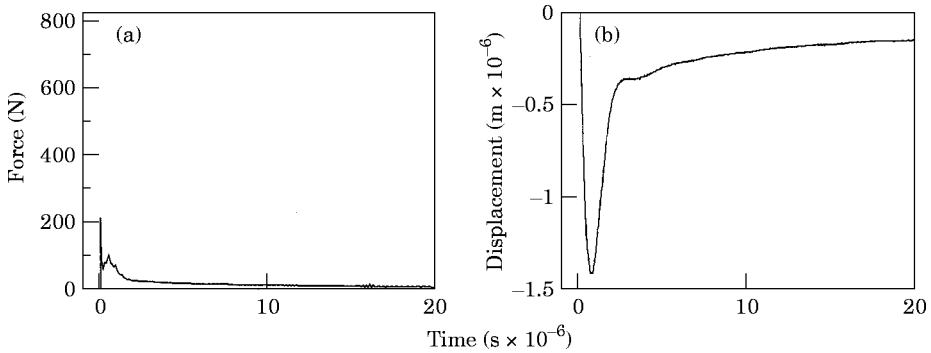

Figure 6. Beam-half space impact, time histories of (a) the contact force and (b) the displacement of the stop at the contact center.

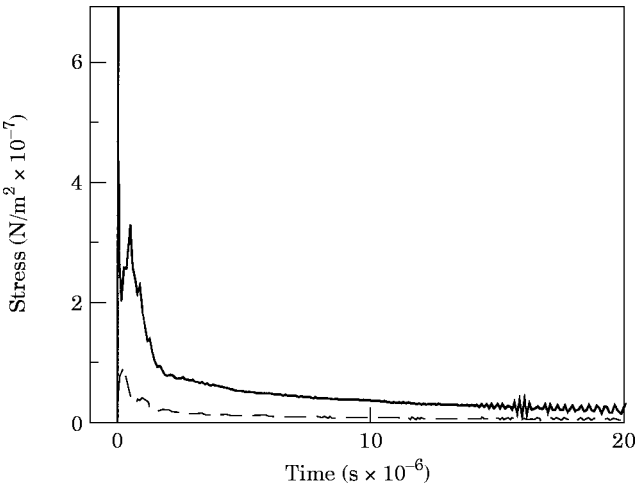

Figure 7. Time histories of the contact pressure: ——, when the contact radius is taken as 2 mm; – – –, when the contact radius is taken as 1 mm.

contact center, the calculated response of the system becomes much less dependent on the assumed contact area.

The phenomenon mentioned above occurs because the spatial and temporal distributions of the contact pressure tend to change in opposite directions as the assumed contact area changes. That is, the calculated contact pressure time history becomes a narrow and sharp signal as the assumed contact area, the spatial distribution, becomes wide, and vice versa. The combined effect of the wave propagation to a point far from

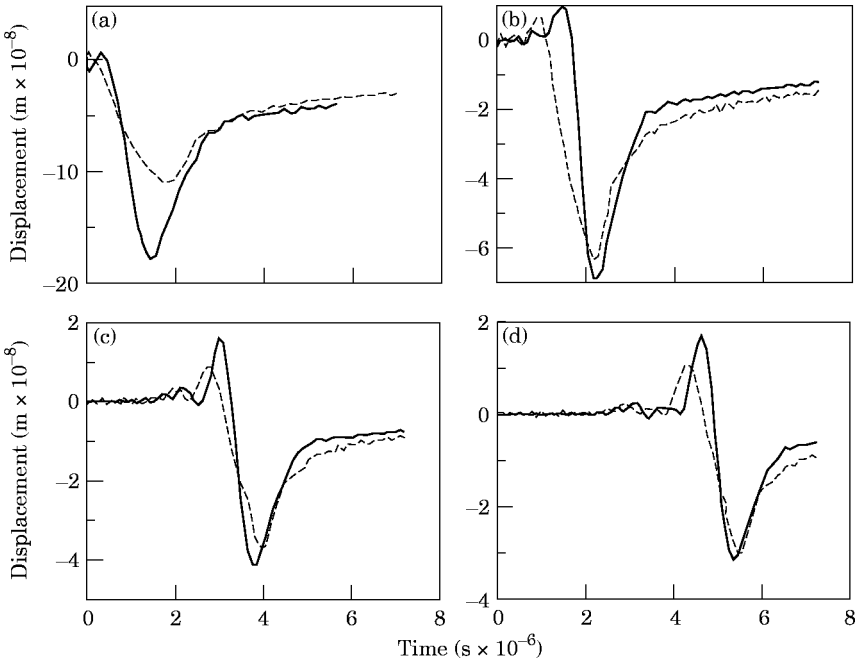

Figure 8. Displacement responses at points away from the contact center by (a) 2·5 mm, (b) 5 mm, (c) 10 mm, (d) 15 mm; ——, when the contact radius is taken as 2 mm; – – –, when the contact radius is taken as 1 mm.

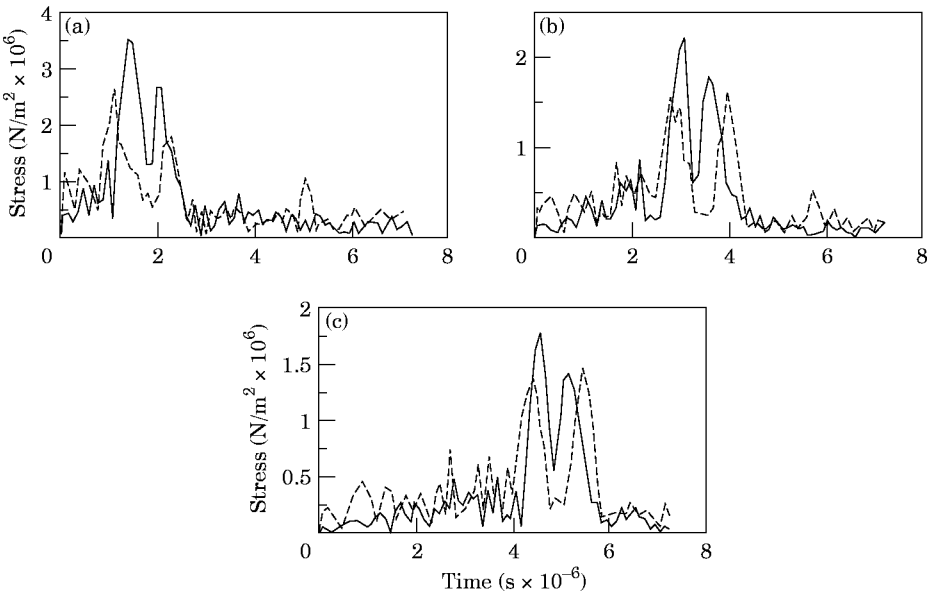

Figure 9. Stress responses at points away from the contact center by (a) 5 mm, (b) 10 mm, (c) 15 mm; ——, when the contact radius is taken as 2 mm; – – –, when the contact radius is taken as 1 mm.

the contact center makes the response at the point depend much less on the size of the assumed contact area than at a point close to the contact center. This may be understood as a dynamic version of the Saint-Venant's principle. Therefore, the proposed procedure would provide a reliable method to estimate the impact response of the system except for the points at the vicinity of the contact center.

5. IMPACT OF THE BEAM AGAINST STOPS OF VARIOUS GEOMETRY

Figure 10 shows the geometry of two possible designs of the stop. The stop in Figure 10(a) resembles a one-dimensional rod. Figure 10(b) shows a finite thickness plate used as a stop. Material properties of the stops and the beam, the dimensions of the beam, and the initial beam deflection are as in section 4. The radius of the contact circle is 1 mm for all the cases discussed in this section.

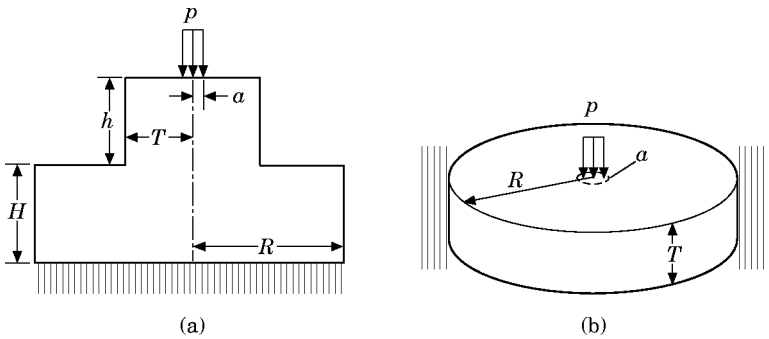

Figure 10. Stops of two different geometries: (a) rod-like stop, (b) finite thickness circular plate.

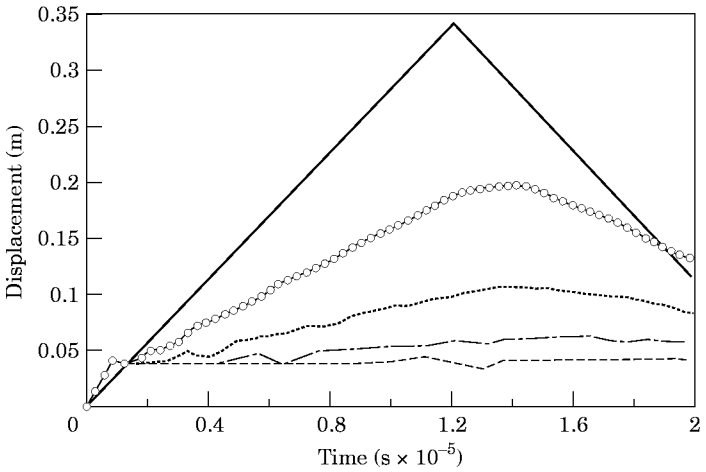

Figure 11. Unit step response of the rod-like stop for various geometries: T/a values: ——, 1 (exact solution); –○–○–, 2; · · · ·, 3; — — — —, 5; — — —, 10.

5.1. ROD-LIKE STRUCTURES

The stop shown in Figure 10(a) has a general shape which resembles a one-dimensional rod of a circular cross-section. Referring to the figure, $h = 30$ mm, $R = 30$ mm, and $H = 30$ mm. Figure 11 shows the unit step responses of such a structure for five different cross-sectional areas, $T/a = 1, 2, 3, 5, 10$, where T is the radius of the cross-section and a is the radius of the contact circle fixed as 1 mm. The exact unit step response of a one-dimensional rod taken from reference [1] is also included in the figure. As expected, the response of the stop becomes very similar to that of the one-dimensional rod as the ratio T/a approaches 1 and the response of the stop becomes similar to that of the half

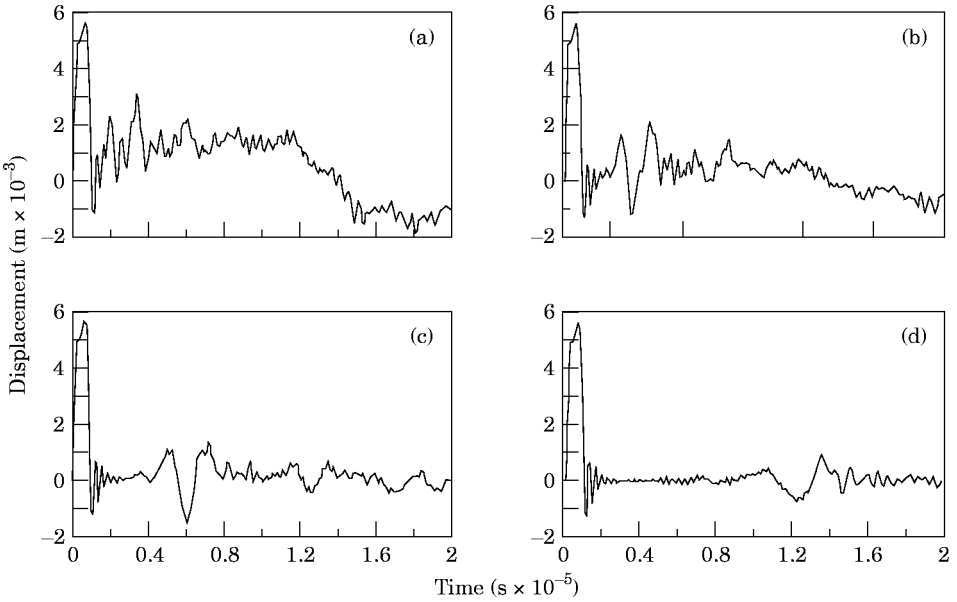

Figure 12. Contact response time histories of the system with a rod-like stop: T/a values: (a) 2, (b) 3, (c) 5, (d) 10.

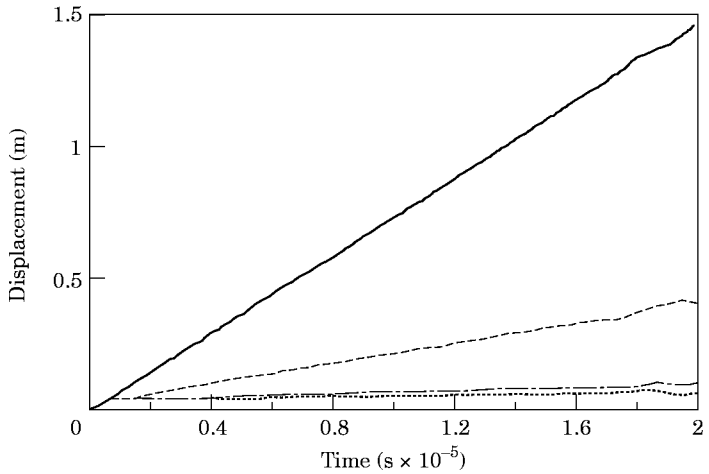

Figure 13. Using step responses of the circular plates of various thickness: T/a values: ——, 1; — — —, 2; — – — –, 5; · · · ·, 7.

space as the ratio T/a increases. Judging from these step responses, it is expected that the impact response of the system will show a similar tendency.

Figure 12 shows the time histories of the contact force and displacements obtained for the five different cases. In all cases, the maximum contact force arises immediately after the contact begins and exhibits a similar magnitude, which is expected because the waves reflected from the free surfaces do not come back to the contact point at the very early stage of the contact. Time histories of the displacement response and the contact force at the later stage are quite different from one case to another. The responses at the early stage of the contact become similar to that of the system with a half space stop, then diverge to different forms as time progresses.

5.2. CIRCULAR PLATE

A circular plate whose radius R is 60 mm has a clamped boundary along the edge as shown in Figure 10(b). The edge boundary condition has virtually no effect on the impulse response of the plate because the amplitude of the impact response of the system becomes almost insignificant by the time the wave travels back to the contact point after reflection from the edge.

Step responses of the plate of different thickness are shown in Figure 13 for $T/a = 1, 2, 3, 5, 10$, where T is the thickness of the plate and a is the radius of the contact circle fixed as 1 mm. As expected, the impulse response becomes very close to that of the half space as the plate becomes thicker. Figure 14 shows the time histories of the contact force and displacements for different T/a ratios.

6. SUMMARY AND CONCLUSIONS

Contact problems of a thin beam impacting against stops of various three-dimensional geometry were solved by extending the procedure developed earlier by the authors [1]. For the impulse response functions of the beam and the stop required to use the procedure, an analytical solution was used for the beam response function and a FEM solution was used for the stop. An efficient method to obtain the FEM based impulse response function was discussed with examples. While the size of the contact area has to be assumed in the procedure, investigation of the impact responses of the system with various different

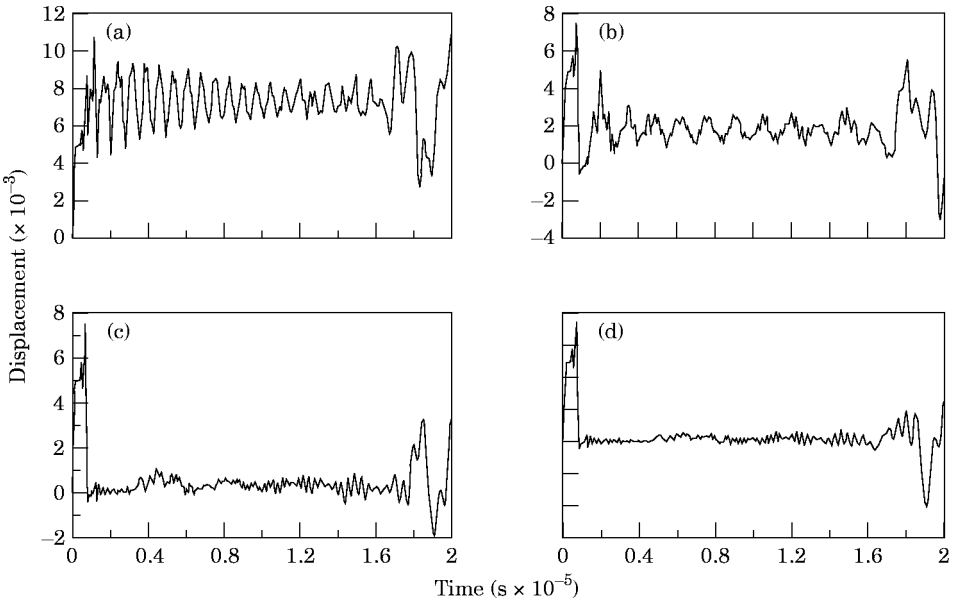

Figure 14. Contact response time histories of the system with a circular plate of various thickness as the stop: T/a values: (a) 1, (b) 2, (c) 5, (d) 7.

assumed contact areas revealed that the response of a point far from the center of the contact is influenced only slightly by the assumed area. This may be viewed as a dynamic version of the Saint-Venant's principle. Therefore, the impact responses of the system can be simulated in a self contained manner by the proposed procedure except for the response of a point right at the vicinity of the contact center which is not a major concern in practical applications, because most impact related failures occur along the free edge of the beam.

The analysis procedure was applied to the systems with two other types of stops of more realistic geometry. It was shown that their impact responses are similar to that of the system with a half space stop at the earlier stage of the contact. If wave reflecting surfaces are located relatively far from the contact point, the intensity of the impact response at the contact point decays to an insignificant level by the time the first reflected wave arrives at the contact point. Therefore, modelling the stop as the half space will provide accurate results for such cases.

The main contribution of this work is that a self-contained analysis method has been developed to calculate dynamic responses of a thin beam impacting against a stop of general three-dimensional geometry. One possible extension of the current work is considered to be employing a two step analysis for the design of reed valves and stops in practical machines. Utilizing the procedure developed in this work, the impact force time history can be calculated as the first step. Idealizing the stop as a half space will simplify the procedure substantially for many practical geometries because it will provide the impact force time history accurate for the time duration while the force is at a level of actually significant magnitude. By modelling the stop as a half space, calculation of the impulse response function of the stop, which is the most time consuming part when using the procedure, can be avoided. Then, as the second step the stress wave propagation in the stop or beam structure may be solved using its actual geometry and the impact force time history obtained in the first step.

REFERENCES

1. C. Wang and J. Kim 1996 *Journal of Sound and Vibration* **191**, 809–823. New analysis method for a thin beam impacting against a stop based on the full continuous model.
2. A. Fathi and N. Popplewell 1994 *Journal of Sound and Vibration* **170**, 365–375. Improved approximations for a beam impacting a stop.
3. C. Lo 1980 *Journal of Sound and Vibration* **60**, 245–255. A cantilever beam chattering against a stop.
4. R. J. Rogers and R. J. Pick 1976 *Nuclear Engineering and Design* **36**, 81–90. On the dynamic spatial response of a heat exchanger tube with intermittent baffle contacts.
5. J. Blinka 1984 *Ph.D. Thesis*, *Purdue University*. A numerical method for the analysis of stress wave propagation in elastic solids.
6. J. S. Kim and W. Soedel 1988 *Journal of Sound and Vibration* **126**, 279–295. On the response of three-dimensional elastic bodies (compressor valves) to distributed dynamic pressures, Part 1: half space.
7. J. S. Kim and W. Soedel 1988 *Journal of Sound and Vibration* **126**, 296–308. On the response of three-dimensional elastic bodies (compressor valves) to distributed dynamic pressures, Part 2: thick plate.
8. S. P. Timoshenko and J. N. Goodier 1975 *Theory of Elasticity*. New York: McGraw-Hill; third edition.